

7-3-2007

# Characterization and Structure of a Zn<sup>2+</sup> and [2Fe-2S]-containing Copper Chaperone from *Archaeoglobus Fulgidus*

Matthew H. Sazinsky  
*Northwestern University*

Benjamin LeMoine  
*Northwestern University*

Maria Orofino  
*Worcester Polytechnic Institute*

Roman Davydov  
*Northwestern University*

Krisztina Z. Bencze  
*Wayne State University*

*See next page for additional authors*

---

## Recommended Citation

Sazinsky, M. H., LeMoine, B., Orofino, M., Davydov, R., Bencze, K. Z., Stemmler, T. L., Hoffman, B. M., Argüello, J. M., and Rosenzweig, A. C. (2007) *J. Biol. Chem.* **282**, 25950-25959. doi:10.1074/jbc.M703311200  
Available at: [http://digitalcommons.wayne.edu/med\\_biochem/5](http://digitalcommons.wayne.edu/med_biochem/5)

This Article is brought to you for free and open access by the Department of Biochemistry and Molecular Biology at DigitalCommons@WayneState. It has been accepted for inclusion in Biochemistry and Molecular Biology Faculty Publications by an authorized administrator of DigitalCommons@WayneState.

---

**Authors**

Matthew H. Sazinsky, Benjamin LeMoine, Maria Orofino, Roman Davydov, Krisztina Z. Bencze, Timothy L. Stemmler, Brian M. Hoffman, José M. Argüello, and Amy C. Rosenzweig

This is the author's post-print version, previously appearing in the *Journal of Biological Chemistry*, 2007 282: 25950-25959.

Available online at: <http://www.jbc.org/>

# Characterization and Structure of a Zn<sup>2+</sup> and [2Fe-2S]-Containing Copper Chaperone from *Archaeoglobus fulgidus*

Matthew H. Sazinsky,<sup>§</sup> Benjamin LeMoine,<sup>§</sup> Maria Orofino,<sup>†</sup> Roman Davydov,<sup>§</sup> Krisztina Z. Bencze,<sup>‡</sup> Timothy L. Stemmler,<sup>‡</sup> Brian M. Hoffman,<sup>§</sup> José M. Argüello,<sup>†,¶</sup> and Amy C. Rosenzweig<sup>§,¶</sup>

From the <sup>§</sup>Departments of Biochemistry, Molecular Biology, and Cell Biology and of Chemistry, Northwestern University, Evanston IL 60208, <sup>†</sup>Department of Chemistry and Biochemistry, Worcester Polytechnic Institute, Worcester MA 01609, <sup>‡</sup>Department of Biochemistry and Molecular Biology, Wayne State University School of Medicine, Detroit, Michigan 48201

Address correspondence to: Amy C. Rosenzweig, Departments of Biochemistry, Molecular Biology, and Cell Biology and of Chemistry, Northwestern University, Evanston IL 60208, Tel.: 847-467-5301; Fax. 847-467-6489; E-mail: [amy@northwestern.edu](mailto:amy@northwestern.edu) and José M. Argüello, Department of Chemistry and Biochemistry, Worcester Polytechnic Institute, Worcester MA 01609, Tel. (508)-831-5326; Fax. (508)-831-5933; E-mail: [arguello@wpi.edu](mailto:arguello@wpi.edu)

## Abstract

Bacterial CopZ proteins deliver copper to P<sub>1B</sub>-type Cu<sup>+</sup>-ATPases that are homologous to the human Wilson and Menkes disease proteins. The genome of the hyperthermophile *Archaeoglobus fulgidus* encodes a putative CopZ copper chaperone that contains an unusual cysteine rich N-terminal domain of 130 amino acids in addition to a C-terminal copper-binding domain with a conserved CXXC motif. The N-terminal domain (CopZ-NT) is homologous to proteins found only in extremophiles and is the only such protein that is fused to a copper chaperone. Surprisingly, optical, electron paramagnetic resonance, and X-ray absorption spectroscopic data indicate the presence of a [2Fe-2S] cluster in CopZ-NT. The intact CopZ protein binds two copper ions, one in each domain. The 1.8 Å resolution crystal structure of CopZ-NT reveals that the [2Fe-2S] cluster is housed within a novel fold and that the protein also binds a zinc ion at a four cysteine site. CopZ can deliver Cu<sup>+</sup> to the *A. fulgidus* CopA N-terminal metal binding domain and is capable of reducing Cu<sup>2+</sup> to Cu<sup>+</sup>. This unique fusion of a redox-active domain with a CXXC-containing copper chaperone domain is relevant to the evolution of copper homeostatic mechanisms and suggests new models for copper trafficking.

Copper is a meticulously regulated redox active micronutrient found in a number of important enzymes, including cytochrome *c* oxidase and superoxide dismutase. Since free or excess intracellular copper can cause oxidative damage, both prokaryotes and eukaryotes have developed specific copper trafficking and transport pathways (1,2). Deficiencies in these processes are linked to human diseases, including Wilson and Menkes disease. In Wilson disease, accumulation of copper in the liver and brain leads to cirrhosis and neurodegeneration, and in Menkes disease, copper transport across the small intestine is impaired, leading to copper deficiency in peripheral tissues (3,4). Both disorders are caused by mutations in Cu<sup>+</sup>-transporting P<sub>1B</sub>-type ATPases (5-7), enzymes that are found in most organisms and function in the cellular localization and/or export of cytosolic copper (8,9).

The Cu<sup>+</sup>-ATPases comprise eight transmembrane (TM) helices, of which three (TM6, TM7, and TM8) contribute invariant residues to form the transmembrane metal binding site, a cytosolic ATP binding domain linking TM6 and TM7, an actuator domain (A-domain) between TM4 and TM5, and cytosolic metal binding domains (MBDs) of ~60-70 amino acids that bind Cu<sup>+</sup> (8,10). Whereas prokaryotic Cu<sup>+</sup>-ATPases typically have one or two MBDs, eukaryotic homologs have up to six such domains. Each MBD contains a highly conserved CXXC consensus sequence for binding Cu<sup>+</sup> and adopts a βαββαβ fold (11-14) nearly identical to that of the Atx1-like cytosolic copper chaperones, including yeast Atx1, human Atox1, and bacterial CopZ (15-19). These chaperones also contain a CXXC motif and deliver Cu<sup>+</sup> to one or all of the MBDs (20-26). It is not clear how Cu<sup>+</sup> reaches the transmembrane metal binding site and how the cytosolic chaperones participate in this process.

The hyperthermophilic Cu<sup>+</sup>-ATPase CopA from *Archaeoglobus fulgidus* is readily expressed in fully active recombinant form, is highly stable, and contains all of the essential structural elements for copper transfer, including one N-terminal and one C-terminal MBD (27-29). CopA is therefore an excellent model system both for investigating the mechanisms of P<sub>1B</sub>-type ATPases and for studying interactions between a cytosolic chaperone and its intact partner Cu<sup>+</sup>-ATPase. The only potential copper chaperone protein in the *A. fulgidus* genome, which we have designated *A. fulgidus* CopZ, differs from all other known copper chaperones in that it contains an additional 130 amino acids fused to the N-terminus of a 60 residue CXXC-containing sequence that is homologous to Atx1-like chaperones and Cu<sup>+</sup>-ATPase MBDs (Fig. 1A). Notably, the *A. fulgidus* CopA C-terminal metal binding domain (CopA C-MBD) is the most similar to the CopZ C-terminus, with 42% identity. The CopA N-terminal MBD (CopA N-MBD) is only 20% identical to CopZ. The novel N-terminal domain of CopZ (CopZ-NT) contains 9 conserved cysteine residues and resembles uncharacterized 10-15 kDa

**Characterization and Structure of a Zn<sup>2+</sup> and [2Fe-2S]-Containing Copper Chaperone from *Archaeoglobus fulgidus* | Matthew Sazinsky, et. al**

proteins from other extremophilic archaea (Fig. 1B). The *A. fulgidus* protein is the only one in which this domain is fused to a putative copper chaperone, however. In all the other extremophilic organisms that have a CopZ-NT homolog, the putative copper chaperone exists as a separate 70 amino acid protein, and its gene is not located in an operon with that encoding a CopZ-NT homolog, suggesting that their expression might not be linked.

Here we describe the characterization and 1.8 Å resolution crystal structure of the *A. fulgidus* CopZ N-terminus (CopZ-NT). Surprisingly, CopZ-NT contains a [2Fe-2S] cluster and a mononuclear zinc site. The fusion of a redox-active domain with a CXXC-containing copper chaperone is unprecedented and suggests previously unrecognized paradigms for copper trafficking and regulation.

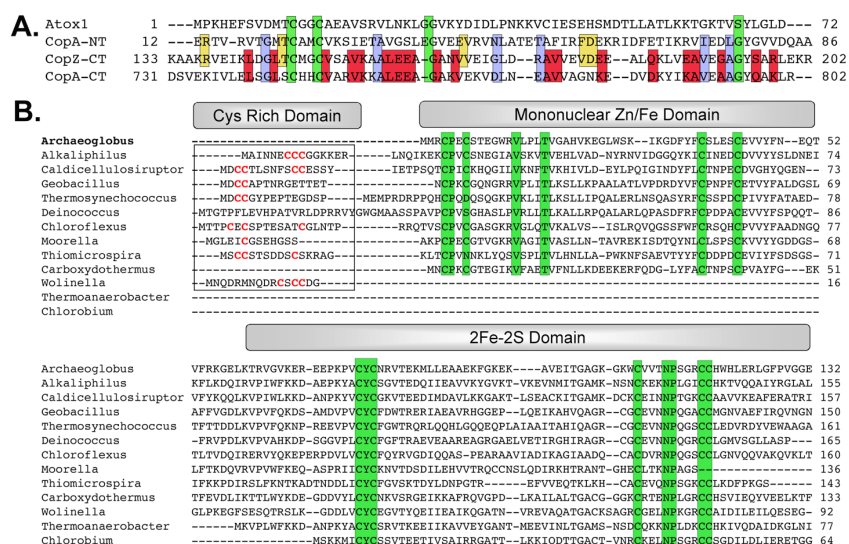


Fig. 1 Sequence alignment of the *A. fulgidus* CopZ domains. (A) CopZ C-terminal domain sequence alignment to the *A. fulgidus* CopA N- and C-terminal MBDs, and to human Atox1. Completely conserved residues are highlighted green, residues conserved among the *A. fulgidus* proteins are highlighted blue, residues conserved between CopZ-CT and CopA-NT are highlighted yellow, and residues conserved between CopZ-CT and CopA-CT are highlighted red. (B) N-terminal domain sequence alignment. Sequences of homologous proteins used for the alignments were from the following species: *Archaeoglobus fulgidus* DSM 4304 (NP\_069182.1), *Alkaliphilus metalliredigenes* QYMF (EAO82573.1), *Caldicellulosiruptor saccharolyticus* DSM 8903 (EAP42583.1), *Carboxydotherrmus hydrogenoformans* Z-2901 (YP\_359666.1), *Moorella thermoacetica* ATCC 39073 (YP\_429978.1), *Deinococcus geothermalis* DSM 11300 (ZP\_00398040.1), *Geobacillus kaustophilus* HTA426 (YP\_146024.1), *Chloroflexus aurantiacus* J-10-fl (EAO58988.1), *Thermoanaerobacter tengcongensis* MB4 (NP\_623988.1), *Thiomicrospira crunogena* XCL-2 (YP\_392381.1), *Thermosynechococcus elongatus* BP-1 (NP\_682675.1), *Chlorobium tepidum* TLS (NP\_662049.1), *Wolinella succinogenes* DSM 1740 (NP\_906973.1). The protein accession numbers are in parentheses.

## Materials and Methods

*Cloning and Purification of CopZ and the CopA N-terminal MBD.* The gene encoding CopZ (AF0346) was cloned from *A. fulgidus* genomic DNA by PCR using the primers 5'-ATGATGCGATGCCAGAAATG-3' and 5'-TCTCTTTCAAGCCGTGCAGA-3'. The purified gene and the plasmid pPRIBA1 (IBA, Germany) were digested with the restriction enzyme *BsaI*, purified, and ligated to create the plasmid pCOPZ, which fuses a 10 amino acid (SAWSHPQFEK) streptactin tag to the C-terminus of the expressed gene product. The gene encoding CopZ was also cloned into pBAD/TOPO vector (Invitrogen, Carlsbad, CA) using the primers 5'-ATGATGCGATGCCAGAAATG-3' and 5'-TCTCTTTCAAGCCGTGCAGA-3' to attach a (His)<sub>6</sub>-tag to the CopZ N-terminus. The N-terminal domain of CopZ (residues 1-131, CopZ-NT) was PCR amplified from the pCOPZ plasmid by using the primers 5'-CGGGAAGGTCTCTGCGCTTCCAACGGG-AAATCC-3' and 5'-GCCCTTGGTCTCTAATGATCGATGCCAGAAAT-3', which encode for a *BsaI* restriction site. As described above, the gene was inserted into the pPRIBA1 plasmid to create pCOPZNT. The C-terminal CXXC-containing copper chaperone domain (residues 132-204, CopZ-CT) was PCR amplified from the pCOPZ plasmid to include the streptactin tag by using the primers 5'-GGAATTCATATGGGTGAGAAGAAAGCGGCTAAAAG-3' and 5'-CCGCTCGAGTTATTTTCGAACTGCGGGTGGCTCCAAGC-3', which incorporate a 5' *NdeI* and 3' *XhoI* restriction sites. The purified gene product and a pET21b plasmid (Novagen) were digested, purified, and combined to create the pCOPZCT vector. The CopA N-MBD (residues 16-87) was cloned into a pASK-IBA3 vector after PCR amplification with the primers 5'-GCCCTTGGTCTCTAATGGAAAGAACCGTCAGAGTTAC-3' and 5'-CGGGAAGGTCTCTGCGCTAGCAGCTTGCTCATCCACCACAC-3' as described above to create the construct pCOPANT.

BL21Star(DE3)pLysS *E. coli* cells carrying the plasmid pSJS1240 encoding for rare tRNAs (tRNA<sup>arg</sup>AGA/AGG and tRNA<sup>ile</sup>AUA) were transformed with the pCOPZ and pCOPZNT, and pCOPANT constructs. BL21(DE3)pLysS *E. coli* cells (Stratagene) were transformed with the pCOPZCT plasmid and the (His)<sub>6</sub>-tagged CopZ construct was inserted into *E. coli* TOP10CP cells. All cell types were grown in Luria-Bertani media at 37 °C in the presence of 100 mg/l carbanicillin and 20 mg/l chloramphenicol. Media for cells harboring the pSJS1240 plasmid were supplemented with 70 mg/l spectinomycin. At an OD<sub>600</sub> of ~0.6-0.7, protein expression was induced by adding either 100-500 μM isopropyl β-D-thiogalactopyranoside to cells containing the pPRIBA1 and pET21 vectors, 200 μg/L tetracycline to cells containing the pASK-IBA3 vector or 0.02% arabinose to cells

expressing (His)<sub>6</sub>-tagged CopZ from the pBAD/TOPO vector. For cells expressing CopZ or CopZNT, 100 μM ferrous ammonium sulfate was added to the media at induction and every hour thereafter. The cells were harvested by centrifugation at 6000 x g for 5 min 3-4 h after induction. The pellet was washed with 25 mM Tris-HCl, pH 7.0, 100 mM KCl, frozen in liquid nitrogen and stored at -80 °C until further use. Full length CopZ was also expressed as described above in cells grown in minimal media supplemented with 100 μM iron ammonium sulfate that contained less than 10 μM zinc.

Streptactin-tagged CopZ, CopZ-NT, CopZ-CT, and the CopA N-MBD were purified by using a procedure identical to the one described for the *A. fulgidus* CopA ATP binding domain (29) except that 1 mM DTT was added to all of the buffers. The (His)<sub>6</sub>-tagged CopZ was purified on a Ni-NTA column (Invitrogen, Carlsbad, CA) following the manufacturer's instructions. The purified protein was either exchanged into 20 mM MOPS, pH 7.0, 20 mM NaCl, 1 mM DTT, 5% glycerol by several concentration and dilution steps using an Amicon Ultra YM-10 or YM-5 concentrator or into 25 mM Tris-HCl, pH 8.0, 50 mM NaCl, 1 mM DTT by using a Sephadex G-25 column. The proteins was frozen at 30 mg/ml in liquid nitrogen, and stored at -80 °C until further use. Protein concentrations were estimated by using the Bradford assay (Sigma).

*Site-Directed Mutagenesis.* Site-directed mutagenesis was performed by using the Quick Change method (Stratagene) and the pCOPZ vector. The DNA primers for 9 single Cys to Ser mutations in the N-terminus are listed in Table 1. Mutations were verified by DNA sequencing. All CopZ mutants were expressed and purified from BL21Star(DE3)pLysS *E. coli* cells containing the pSJS1240 plasmid using the procedures described above.

**Table 1. Oligonucleotide Primers for Site-Directed Mutagenesis of CopZ**

Cys4Ser	5' ATGATGCGAAGCCCAGAATGCAGCACGGAAG
Cys7Ser	5' GATGCCAGAAAAGCAGCACGGAAGGATGGAG
Cys38Ser	5' GGATTTTACTTCAGCTCTTTGGAGAGCTGCGAGG
Cys43Ser	5' CTGCTCTTTGGAGAGCAGCGAGGTTGTTTACTTC
Cys75Ser	5' CAAAGCCGGTTAGCTACTGCAACAGGGTTACAGAG
Cys77Ser	5' CAAAGCCGGTTTGCTACAGCAACAGGGTTACAGAG
Cys109Ser	5' CAGGAAAAGGAAAATGGAGCGTCGTTACCAACCCATC
Cys118Ser	5' CATCCGGGAGAAGCTGCCACTGGCATCTGG
Cys119Ser	5' CATCCGGGAGATGCAGCCACTGGCATCTGG

*Metal Binding Analysis.* Apo forms of the proteins were loaded with Cu<sup>+</sup> by incubation with a 10 molar excess of CuCl<sub>2</sub> or CuSO<sub>4</sub> in 25 mM Tris-HCl, pH 8.0, 50 mM NaCl, 1 mM DTT or 25 mM

MOPS, pH 7.0, 25 mM NaCl, 5 mM DTT for 10-60 min at room temperature with gentle agitation. The unbound copper was removed by centrifuging in a 10 kDa cutoff centricon Amicon-15 (Millipore, MA) after diluting the sample with 15-20 volumes of buffer without DTT or desalting over a PD-10 column (BioRad).

The amount of bound copper was determined by the BCA method (30). Briefly, the proteins were precipitated by mixing up to 55  $\mu$ l of sample with 18.3  $\mu$ l of 30% TCA. The pellet was separated by centrifugation for 5 min at 9,000 x g. The supernatant (66  $\mu$ l) was mixed with 5  $\mu$ l of 0.07% freshly prepared ascorbic acid and 29  $\mu$ l of 2x BCA solution (0.012% BCA, 7.2% NaOH, 31.2% HEPES). After a 5 min incubation at room temperature, the absorbance at 359 and 562 nm was measured. CuCl<sub>2</sub> solutions were used as standards. Concentrations of 2-10  $\mu$ M Cu<sup>+</sup> were within the linear range.

The iron content was determined by using a ferrozine assay (31), and acid-labile sulfide was quantified by using the method of Beinert (32). Zinc content was determined by flame atomic absorption spectrometry (AAS) and by ICP atomic emission spectrometry. The results of three measurements were averaged and the concentration was determined from a standard curve.

The presence of various metal ions was also investigated by using X-ray fluorescence spectroscopy at the sector 5 beamline at the Advanced Photon Source. A small sample of 2 mM CopZ in 25 mM Tris pH 7.5, 100 mM NaCl, 5% glycerol was frozen at 100 K on a standard protein crystal mounting loop and exposed to X-rays tuned to the absorption edges of Fe, Co, Ni, Cu, Ni, Zn, and W.

*Cu<sup>+</sup> transfer between CopZ and the CopA N-MBD.* Apo-CopA N-MBD was incubated with streptactin beads in a column for 20 min at room temperature with gentle agitation. To separate unbound protein, the column was washed with 10 volumes of buffer W (25 mM Tris-HCl, pH 8.0, 150 mM NaCl, 10 mM ascorbic acid). (His)<sub>6</sub>-tagged CopZ loaded with 1.8 +/- 0.1 Cu<sup>+</sup> was added in 6.6 fold excess to the column containing bound CopA N-MBD and incubated for 10 min at room temperature to initiate copper exchange. The proteins were then separated by washing the column with 10 volumes of buffer W followed by elution of the CopA N-MBD with buffer W containing 2.5 mM 2-(4-hydroxyphenylazo)benzoic acid (HABA). Both the wash and elution fractions were collected and analyzed for copper and protein content. To confirm that only the CopA N-MBD was present in the elution fractions, each fraction was analyzed by SDS-PAGE. As a control, copper-loaded CopZ was incubated with streptactin beads without bound CopA N-MBD was subjected to the procedure described above and demonstrated no copper loss. Streptactin-bound apo CopA N-MBD incubated with just buffer W did not acquire copper either.

*Reduction of Cu<sup>2+</sup> by CopZ.* Under anaerobic conditions, 1 mM CopZ and CopZ-NT in 25 mM MOPS, pH 7.0, 25 mM NaCl were reduced with four-fold excess dithionite and desalted on a PD-10 column (BioRad) equilibrated with 50 mM Tris pH, 7.0, 50 mM NaCl. A ten-fold excess of BCA and a three-fold excess of CuSO<sub>4</sub> was then added to the eluted protein and allowed to incubate for 4 hr at 25 °C to detect the reduction of Cu<sup>2+</sup> to Cu<sup>+</sup> colorimetrically. As a control, 1 mM CopZ and CopZ-NT in 25 mM MOPS, pH 7.0, 25 mM NaCl were oxidized with 10 mM K<sub>3</sub>Fe(CN)<sub>6</sub> under aerobic conditions, desalted, moved into the anaerobic chamber, and incubated with BCA and CuSO<sub>4</sub> as described above. No color change was observed.

*X-ray Absorption Spectroscopy.* XAS samples were prepared anaerobically and aerobically for reduced and oxidized CopZ and CopZ-NT. Multiple independent but reproducible samples were prepared at 2.0-5.0 mM iron concentrations in 100 mM Tris, pH 8.0, 150 mM NaCl, 30% glycerol and transferred into Lucite sample cells wrapped with Kapton tape. Samples were immediately frozen in liquid nitrogen. Iron XAS data for full-length CopZ were collected at Brookhaven National Laboratory (NSLS) beamline X-9B using a Si-(111) crystal monochromator equipped with a harmonic rejection mirror. Samples were kept at 24 K using a He Displex cryostat, and protein fluorescence excitation spectra were collected using a 13-element Ge solid-state detector. Spectra were collected with a iron foil control in a manner described previously (33). During data collection, each spectrum was closely monitored for photoreduction. The data represent the average of 7-10 scans.

XAS data were analyzed using the the Macintosh OS X version of the EXAFSPAK program suite (34) integrated with the Feff v7.2 software (35) for theoretical model generation. Processing methods and fitting parameters used during data analysis are described in detail elsewhere (33,36). Single scattering theoretical models were used during data simulation. Data were simulated over the spectral  $k$  range of 1 to 12.85 Å<sup>-1</sup>, corresponding to a spectral resolution of 0.13 Å (37). When simulating empirical data, only the absorber-scatterer bond length (R) and Debye-Waller factor ( $\sigma^2$ ) were allowed to freely vary while metal-ligand coordination numbers were fixed at quarter-integer values. The criteria for judging the best fit simulation and for adding ligand environments included a reduction in the mean square deviation between data and fit ( $F^2$ ) (38), a value corrected for number of degrees of freedom in the fit, bond lengths outside the data resolution, and all Debye-Waller factors having values less than 0.006 Å<sup>2</sup>.

*EPR Spectroscopy.* Dithionite-reduced and as-isolated 2 mM CopZ and CopZ-NT samples in 100 mM Tris (pH 7.0 –10.0), 150 mM NaCl, 20-30% glycerol were frozen in liquid nitrogen in 3 mm i.d.

quartz EPR tubes. Cryoreduction was achieved by  $\gamma$ -irradiation of the samples by exposure to a <sup>60</sup>Co source at a dose rate of 0.46 Mrad h<sup>-1</sup> for 5-10 min. Cryogenically reduced samples were annealed in cooled isopentane at various times and temperatures before being rapidly cooled to 77 K. X-band EPR spectra were recorded between 2-20 K on Bruker ESP300 or EMX spectrometers equipped with an Oxford Instrument ESR900 liquid helium cryostat.

*Structure Determination of the CopZ N-terminus.* CopZ-NT was crystallized in a Coy anaerobic chamber at room temperature by using the sitting drop vapor diffusion method. Equal volumes of protein at ~15 mg/ml in 20 mM MOPS, pH 7.0, 20 mM NaCl, 5% glycerol, 1 mM DTT were combined with a crystallization buffer comprising 100 mM sodium acetate, pH 4.6, 200 mM ammonium sulfate, 15-20% PEG 2000 MME. Dark red crystals grew within two days. The crystals were flash frozen aerobically in a cryosolution consisting of 75 mM sodium acetate, pH 4.6, 100 mM ammonium sulfate, 20% PEG 2000 MME, 20% glycerol. Native and iron anomalous data were collected at 100 K to 2.3-1.8 Å resolution at the Advanced Photon Source on the sector 19 and 23 beamlines (Table 2).

After data collection, sections of the crystal exposed to the X-ray beam turned yellow, suggestive of photoreduction. The crystals belonged to the space group  $P2_12_12_1$  and had unit cell dimensions of  $a = 56.25$ ,  $b = 64.50$ ,  $c = 84.15$ . Data sets were indexed and scaled with HKL2000 (39), and SOLVE (40) and CNS (41) were used to locate 4 iron atoms and calculate phases by the SAD method. After density modification, ARP/wARP was used for automatic model building (42). The remainder of the model was built with XtalView (43) and refined with CNS. Residues 1-130 were observed in one molecule in the asymmetric unit, and residues 2-130 were observed in the second molecule. A Ramachandran plot calculation with PROCHECK (44) indicated that 90% of the residues have the most favored geometry, and the rest occupy additionally allowed regions. The root mean square difference (r.m.s.d.) for backbone atoms between the two molecules in the asymmetric unit is 0.3 Å, and no significant structural differences are observed.

**Table 2.** Data Collection, Phasing and Refinement Statistics

<b>Data Collection</b>	<b>Iron Peak</b>	<b>Native</b>
APS Beamline	GM/CA-CAT (Sector 23)	SBC-CAT (Sector 19)
Wavelength (Å)	1.74	0.979
Resolution (Å) <sup>a</sup>	40.0-2.3	50.0-1.78
Unique Observations	13,948	29,750
Total Observations	195,626	194,503
Completeness (%)	100 (100)	98.9 (93.3)
Redundancy	14.0 (14.0)	6.5 (4.6)
I/σ	19.4 (19.3)	13.0 (3.2)
R <sub>sym</sub> <sup>b</sup> (%)	6.8 (16.8)	6.3 (45.1)
Fe Sites used for phasing	4	
Fig. of merit (after density modification)	0.374 (0.897)	
Refinement		
R <sub>work</sub> (%) <sup>c</sup>		20.9
R <sub>free</sub> (%) <sup>d</sup>		23.5
Molecules in ASU		2
Number of protein-nonhydrogen atoms		2066
Number of protein nonhydrogen atoms		157
R.m.s.d. bond length (Å)		0.0048
R.m.s.d. bond angle (°)		1.14
Average B-value (Å <sup>2</sup> )		37.7

<sup>a</sup>Values in parentheses are for the highest resolution shell (1.84-1.78 Å). <sup>b</sup> $R_{\text{sym}} = \frac{\sum_i \sum_{hkl} |I_i(hkl) - \langle I(hkl) \rangle|}{\sum_i \sum_{hkl} \langle I(hkl) \rangle}$ , where  $I_i(hkl)$  is the  $i^{\text{th}}$  measured diffraction intensity and  $\langle I(hkl) \rangle$  is the mean of the intensity for the Miller index (hkl). <sup>c</sup> $R_{\text{work}} = \frac{\sum_{hkl} | |F_o(hkl)| - |F_c(hkl)| |}{\sum_{hkl} |F_o(hkl)|}$ . <sup>d</sup> $R_{\text{free}} = R_{\text{work}}$  for a test set of reflections (5%).

## Results and Discussion

*Metal Content of CopZ.* Purified CopZ and CopZ-NT are 23 kDa and 14 kDa monomers, respectively, that have a distinct red color whereas the 9 kDa CopZ-CT is colorless. The optical spectra of the full length protein and CopZ-NT are identical with three absorption peaks at 340, 430, 480 nm and a shoulder at 550 nm (Fig. 2A). The spectra are most similar to those observed for [2Fe-2S]-containing proteins (45). Features attributable to either a mononuclear iron center or a [4Fe-4S] cluster are not present. Upon reduction with dithionite, these spectral features disappear. Since the spectra of CopZ and CopZ-NT are identical, it is likely that the C-terminus is not involved in assembly of the CopZ-NT metal centers. Consistent with a [2Fe-2S] cluster, both CopZ and CopZ-NT bound  $1.7 \pm 0.3$  iron ions per protein molecule. Full length CopZ contained  $\sim 0.6$  equivalents of zinc, and the isolated CopZ, CopZ-NT, and CopZ-CT did not contain copper. Only zinc and iron were detected by X-ray fluorescence spectroscopy.

*Copper Binding, Transfer, and Reduction.* After incubation with excess CuSO<sub>4</sub> and DTT and buffer exchange, CopZ, CopZ-NT, and CopZ-CT were determined to bind  $2.1 \pm 0.3$ ,  $1.4 \pm 0.3$ , and  $1.0 \pm 0.4$  Cu<sup>+</sup> ions/protein, respectively. Thus, each domain binds a single Cu<sup>+</sup> ion. Like all of the other Atx1-like proteins, CopZ-CT likely binds Cu<sup>+</sup> via the conserved cysteines in the CXXC motif (vide infra). The presence of a Cu<sup>+</sup> ion bound to CopZ-NT is unexpected.

Copper transfer from (His)<sub>6</sub>-tagged CopZ to the CopA N-MBD was demonstrated by incubating Cu<sup>+</sup>-loaded chaperone with streptactin resin containing bound apo CopA N-MBD, separating the individual proteins, and analyzing the copper content (Fig. 3). The CopA N-MBD was selected for these experiments because mutagenesis data indicate that the N-MBD, but not the C-MBD, is important for CopA activity (46). (His)<sub>6</sub>-tagged CopZ bound  $2.0 \pm 0.1$  copper ions per protein, similar to the value obtained for streptactin-tagged CopZ. Thus, the (His)<sub>6</sub>-tag likely does not interfere with Cu<sup>+</sup> binding. When eluted from the column, 34.5% of the CopA N-MBD was loaded with copper. In control experiments, copper-loaded CopZ incubated with streptactin beads and treated as above did not release copper and retained its full complement. Likewise, streptactin-bound apo CopA N-MBD did not acquire copper after washing and elution steps in the absence of CopZ. Because there is no apparent copper loss or gain in the control experiments, CopZ is therefore capable of delivering Cu<sup>+</sup> to the CopA N-MBD, similar to what has been reported for yeast and human Atx1-like chaperones and their cognate Cu<sup>+</sup>-ATPases (24,25,47). However, when comparing Cu<sup>+</sup> transfer in these various systems, the 80-100 °C optimal growth conditions of *A. fulgidus* should be considered. Thus, a temperature dependence of  $K_{ex}$  might explain the reduced Cu<sup>+</sup> transfer

Characterization and Structure of a Zn<sup>2+</sup> and [2Fe-2S]-Containing Copper Chaperone from *Archaeoglobus fulgidus* | Matthew Sazinsky, et. al

(34.5%) observed in *A. fulgidus* compared to eukaryotic systems (60-90%) (24,25,47) (González-Guerrero and Argüello, unpublished results).

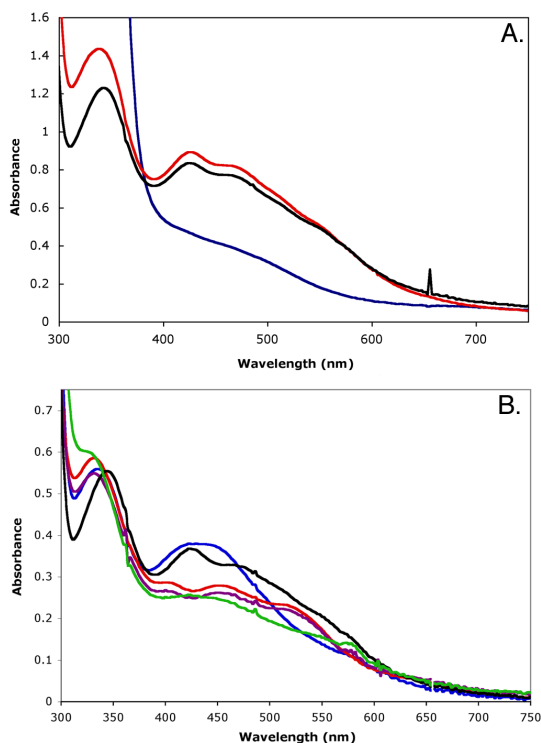


Fig. 2 UV-Vis absorption spectra of CopZ, CopZ-NT, and Cys-to-Ser mutants. (A) Spectra of wild-type (black), dithionite reduced wild-type (blue), and CopZ-NT (red). (B) Spectra of Cys75Ser (red), Cys77Ser (blue), Cys109Ser (purple), Cys118Ser (black), and Cys119Ser (green) variants. All spectra were recorded on 60-80  $\mu$ M protein in 25 mM MOPS, pH 7.0, 25 mM NaCl at room temperature on a Hewlett Packard 8452A diode array spectrophotometer. Anaerobic measurements were obtained by using a custom designed Thünberg cuvette.

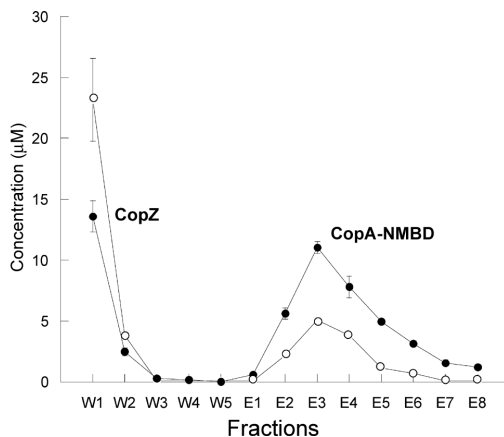


Fig. 3 Copper transfer from CopZ to the CopA N-MBD. The copper (○) and protein (●) content of the wash (W) and elution (E) fractions are shown. Peaks corresponding to specific proteins eluted from the streptatcin column are identified on the Figure. At the end of the experiment, 34.5% of the CopA N-MBD was loaded with copper.

To test whether CopZ and CopZ-NT can reduce Cu<sup>2+</sup> to Cu<sup>+</sup>, chemically oxidized and reduced protein were incubated with CuSO<sub>4</sub> and bicinchoninic acid (BCA), a Cu<sup>+</sup> specific chelator. A magenta Cu<sup>+</sup>-BCA complex was only observed when reduced CopZ and CopZ-NT were added to the CuSO<sub>4</sub>/BCA solution (data not shown). Thus, the *in vitro* reduction of Cu<sup>2+</sup> by the CopZ [2Fe-2S] cluster is favorable and consistent with known redox potentials for Cu<sup>2+</sup>/Cu<sup>+</sup> (154 mV) and [2Fe-2S]<sup>2+</sup>/[2Fe-2S]<sup>+</sup> (200-500 mV) (48). A protein environment, however, can significantly affect the potential of bound copper ions (49), so whether CopZ reduces Cu<sup>2+</sup> *in vivo* would depend on the source of Cu<sup>2+</sup>.

*X-ray Absorption Spectroscopy.* A comparison of the Fe XANES spectra of CopZ in the presence and absence of dithionite is consistent with partial reduction of the [2Fe-2S] cluster. General edge features for the two protein samples differ in their edge first inflection energies (7117.0 eV for reduced and 7117.5 eV for oxidized) as well as a diminished shoulder feature for the oxidized sample at ~7125 eV (Fig. 4A). Features for the 1s→3d pre-edge signal occur at maximal values of 7112.2 eV for the reduced sample and 7112.6 eV for the oxidized sample. Concurrent with a subtle shift in the 1s→3d pre-edge maximal signal energy is an increase in area for this signal from 22.1 to 27.3

(unitless values), consistent with four-coordinate ferrous and ferric iron values obtained from model compounds (50).

Analysis of the EXAFS data for reduced and oxidized CopZ indicates a unique metal-ligand coordination geometry for both samples with trends matching those expected for Fe-S cluster centers in slightly different redox states. The EXAFS of both samples show a node in the scattering oscillations at a  $k$  value of  $7.5 \text{ \AA}^{-1}$ , consistent with destructively interacting distinct ligand environments (Fig.s 4B and 4D). Fourier transforms of the EXAFS data for both samples show two ligand scattering environments at phase shifted bond lengths of  $\sim 1.8 \text{ \AA}$  and  $2.4 \text{ \AA}$ , as well as minimal long range ( $> 3.0 \text{ \AA}$ ) scattering (Fig.s 4C and 4E). Simulations of the iron EXAFS indicate two distinct ligand scattering interactions are present in both samples (Table 3). For the oxidized sample, the data are best fit with ca. 4 Fe-S interactions at  $2.26 \text{ \AA}$  and a single Fe-Fe interaction at  $2.73 \text{ \AA}$ . For the reduced sample, the data are best fit with ca. 4 Fe-S interactions at an extended distance of  $2.29 \text{ \AA}$  and a single Fe-Fe interaction at an extended distance of  $2.77 \text{ \AA}$ . There was no justification for fitting the long range ( $> 3.0 \text{ \AA}$ ) scattering in either data set.

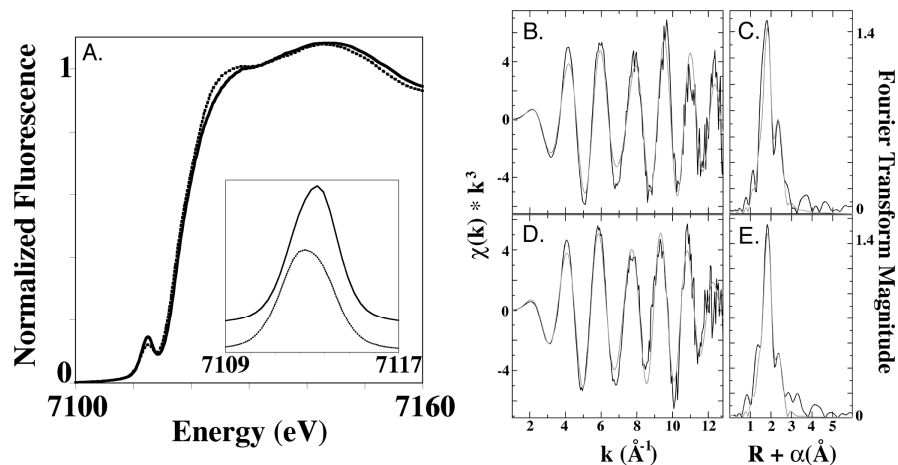


Fig. 4 Iron XAS spectra of CopZ. Normalized XANES spectra for oxidized (solid line) and reduced (dotted line) CopZ samples (panel A). The inset shows the expansion of the background subtracted pre-edge feature for the two samples. The EXAFS and Fourier transforms (FT) of the CopZ iron-sulfur cluster with best fits superimposed in gray for oxidized (panels A and B) and reduced (panels C and D) CopZ samples.

**Table 3.** Summary of Iron EXAFS fitting results for CopZ (Data fit over k range of 1 to 12.85 Å<sup>-1</sup>)

Sample	Fit #	Ligand Environment <sup>a</sup>				Ligand Environment <sup>a</sup>				F <sup>g</sup>
		Ato <sub>m</sub> <sup>b</sup>	R(Å) <sup>c</sup>	C.N. <sup>d</sup>	σ <sup>2</sup> <sup>e</sup>	Ato <sub>m</sub> <sup>b</sup>	R(Å) <sup>c</sup>	C.N. <sup>d</sup>	σ <sup>2</sup> <sup>e</sup>	
CopZ-ox	1.1 <sup>g</sup>	S	2.26	3.5	5.8 5					2.20
	1.2 <sup>g</sup>	S	2.26	3.25	5.5 9	Fe	2.73	1.0	3.6 8	1.20
CopZ-red	2.1 <sup>g</sup>	S	2.29	3.5	5.5 8					1.39
	2.2 <sup>g</sup>	S	2.29	3.5	5.6 6	Fe	2.77	0.8	4.8 0	0.89

<sup>a</sup>Independent metal-ligand scattering environment

<sup>b</sup>Scattering atoms: S (Sulfur)

<sup>c</sup>Metal-ligand bond length

<sup>d</sup>Metal-ligand coordination number

<sup>e</sup>Debye-Waller factor in Å<sup>2</sup> x 10<sup>3</sup>

<sup>f</sup>Number of degrees of freedom weighted mean square deviation between data and fit

<sup>g</sup>Fit using only single scattering Feff 7 theoretical models

*EPR Spectroscopy.* As purified, CopZ is EPR silent. The dithionite reduced protein exhibits a 10 K EPR spectrum with two different types of signal (Fig. 5), indicating the presence of two major conformational substates. The first is the signal in the vicinity of g = 2 (~3500 G), which corresponds to an S = ½ ground state of the reduced cluster. Spectra collected over a range of temperature, ~7K – 40K, show that this comprises the signals from two ‘second-tier’ substates with ferredoxin-type, rhombic spectra **g**<sub>1</sub> = [2.06, 1.91, 1.86] (g<sub>av</sub> = 1.94); **g**<sub>2</sub> = [2.04, 1.97, 1.90] (g<sub>av</sub> = 1.97). The second type of signal (the “g = 3” signal) is associated with S > ½; it is axial with g<sub>⊥</sub> = 3.11 and g<sub>∥</sub> < 1.7 (not observed). These values are uncommon for [2Fe-2S]<sup>+</sup> clusters, and the spin state of the cluster is by no means clear. The high-spin signal accounts for ~ 60% of the reduced [2Fe-2S]<sup>+</sup> centers. Varying the pH between 6 and 10 slightly alters both types of spectrum (Fig. 5B).

To investigate the [2Fe-2S] cluster further and to identify the coordinating residues, 9 Cys-to-Ser mutants were generated. All of the purified mutants are red in color, indicating that the [2Fe-2S]-containing domain is assembled and folded. The UV-vis spectra for four Cys mutants, Cys75Ser,

Cys77Ser, Cys109Ser, and Cys119Ser, are different from the wild type spectra whereas Cys to Ser mutations at positions 4, 7, 38, 43 and 118 exhibited UV-Vis spectra identical to the native protein (Fig. 2B). The Cys75Ser, Cys109Ser and Cys119Ser mutations lead to the complete disappearance of the “g = 3” signal (Fig.s 5D-5F). The Cys75Ser and Cys109Ser mutants also collapse the overlapping S = ½ signals into a single axial ferredoxin-like signal with g<sub>av</sub> < 2, whereas the Cys119Ser mutation leaves the S = ½ region of the spectrum as an overlap of two signals (Fig.s 5D-5F). The Cys77Ser mutant exhibits both types of the signal, but both types are slightly altered (Fig. 5C).

It was demonstrated previously that γ-irradiation at 77 K of diamagnetic diiron(III) centers of frozen protein solutions generates a one-electron reduced product trapped in the conformation of the oxidized precursor (51). The species trapped at 77 K relaxes to an equilibrium state during annealing at elevated temperatures (T > 160 K). Such cryo-reduced proteins provide a sensitive EPR probe of the EPR-silent deferric precursors. The EPR spectrum of cryoreduced CopZ (Fig. 5G) shows well-resolved features from the high-spin conformer, at g = 3.0 and 1.9, which differ from those of the equilibrium conformation. The strong g = 2 signal from radiolytically generated radicals partially obscures the region of the signals of the S = ½ conformers. However, comparison with the spectrum of the chemically reduced protein shows that there are features in the cryoreduction spectrum that would be observable if the S = ½ signals were present, and they are not. Thus, the “g = 3” species is the major product of cryo-reduction, suggesting that the diferric cluster exists as only one major substate. The EPR spectrum of the cryoreduced sample annealed at 240 K (not shown) becomes identical to that of the chemically reduced protein (Fig. 5A), showing that the “g = 3” conformational substate can convert to the S = ½ substate.

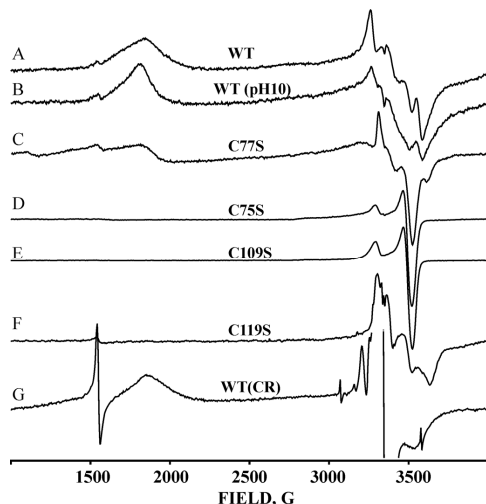


Fig. 5 EPR spectra of CopZ. (A) Chemically reduced CopZ, pH 7.0, (B) Chemically reduced CopZ, pH 10, (C) Cys77Ser variant, (D) Cys75Ser variant, (E) Cys109Ser variant, (F) Cys119Ser variant, (G) After 77K cryoreduction (CR) of diferric CopZ. Sharp feature at ~1500G in some spectra is non-heme Fe(III). The sharp feature at ~1500G in some spectra is non-heme Fe(III). Conditions: T = 10K; frequency, 9.372 GHz; power, 1 mW; modulation amplitude, 5 G.

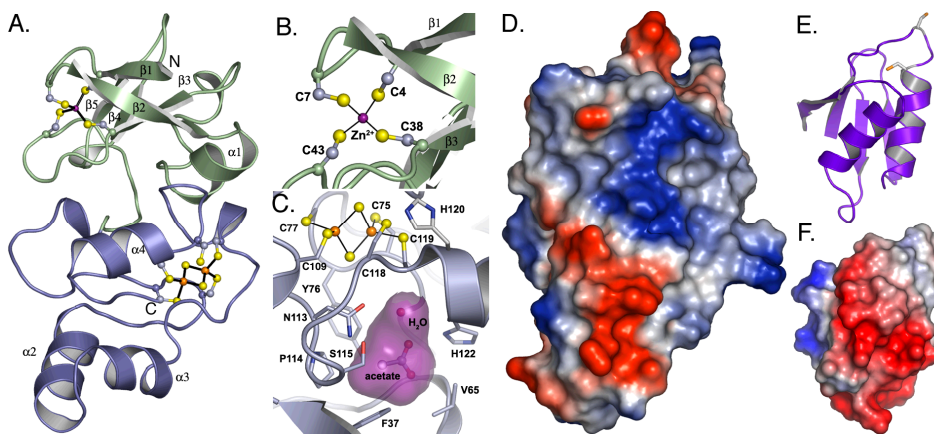


Fig. 6 Crystal structure of CopZ-NT. (A) The N-terminal domain of CopZ-NT is shown in green and the C-terminal domain is shown in blue. The zinc ion is shown as a purple sphere and the [2Fe-2S] cluster is shown as yellow and orange spheres. (B) The [2Fe2S] cluster. Atoms are represented as ball and sticks with carbon in gray, sulfur in yellow and iron in orange. Acetate and water are bound in a small cavity (magenta) directly below the [2Fe-2S] cluster. Residues contributing to the surface of the cavity are shown as ball-and-stick representations. (C) The mononuclear metal center. The zinc ion is shown as a purple sphere. (D) Electrostatic

surface maps of the CopZ-NT and (E) and (F) a homology model of CopZ-CT. The homology model was generated from the PDB file 1OSD by using the CPHmodels server (63). Red surfaces represent regions of negative charge and blue surfaces are positively charged.

*Structure of CopZ-NT.* CopZ-NT is composed of two subdomains, an N-terminal domain containing a mononuclear metal center and a C-terminal domain containing the [2Fe-2S] cluster (Fig. 6A). This distinct domain arrangement is consistent with the observation that the *Wolinella*, *Thermoanaerobacter*, and *Chlorobium* CopZ-NT sequences lack an N-terminal domain (Fig. 1B). Interestingly, other homologs have an additional N-terminal cysteine rich region that is not present in *A. fulgidus* CopZ (Fig. 1B). The folds of the two CopZ-NT subdomains are unique with no similarity to previously determined structures in the PDB according to DALI searches (52).

The N-terminal domain of CopZ-NT has a  $\beta\alpha\alpha\beta\beta\alpha$  fold. The metal ion is coordinated in a tetrahedral arrangement by Cys 4 and Cys 7 on the N-terminal loop before  $\beta 1$  and Cys 38 and Cys 43 on the loop connecting  $\beta 2$  and  $\beta 3$  (Fig. 6B). Of these cysteines, Cys 4, Cys 38, and Cys 43 are conserved among all of the known proteins that have homology to the N-terminus. The *Thiomicrospira*, *Deinococcus*, and *Thermosynechococcus* proteins contain Asn, Ser, and Asp residues, respectively, at position 7 instead of a cysteine (Fig. 1B). The average metal-sulfur distance over both molecules in the asymmetric unit is 2.35 Å. Anomalous difference maps calculated using data collected at the Fe absorption edge yield a small peak at the position of the metal ion (Table 4). This peak is 6-fold less intense than those used to identify the [2Fe-2S] cluster at this wavelength, suggesting that only a trace amount of iron occupies this position. For data collected at the Se absorption edge, the metal ion at this position gives rise to a slightly stronger anomalous signal than the iron atoms in [2Fe-2S] cluster. Based on these anomalous differences, the coordination geometry, and the presence of zinc in the purified protein, it is likely that Zn<sup>2+</sup> primarily occupies this site and that it assumes a structural role in the protein. It is possible that protein purified directly from *A. fulgidus* would contain iron at this position, however. If this were the case, the iron coordination environment would be most similar to that found in rubredoxins (48) and would be consistent with a redox function for this domain. Besides the cysteine ligands, Val 14 from  $\beta 2$  and Thr 18 from  $\alpha 2$  are the only other conserved residues in this domain and may be important for mediating contacts with the [2Fe-2S] domain.

**Table 4.** Anomalous peak heights at the Fe and Se Absorption Edges

Atom	Fe-edge (7177 eV)	Se-edge (13660 eV)
Molecule 1		
Fe1	26.5	10.4
Fe2	25.3	9.3
Zn/Fe	3.9	13.8
Molecule 2		
Fe1	26.5	11.4
Fe2	24.1	8.7
Zn/Fe	3.9	14.5

The [2Fe-2S] domain is all  $\alpha$ -helical and differs significantly from typical [2Fe-2S] ferredoxins, which usually have a  $\beta\alpha\beta\beta\alpha\beta$  fold (53). The [2Fe-2S] center is coordinated by Cys 75, Cys 77, Cys 109, and Cys 119, which are found on loops between the  $\alpha$ -helices (Fig. 6C) and are highly conserved (Fig. 1B). The average Fe-Fe distance of 2.8 Å is nearly identical to the 2.77 Å Fe-Fe distance determined by XAS for reduced CopZ. The average Fe-S(Cys) and Fe-S<sup>2-</sup> distances are 2.35 Å and 2.30 Å, respectively, and the overall geometry of the iron-sulfur cluster is similar to that observed in high resolution crystal structures of [2Fe-2S]-containing proteins (54). The unusual EPR spectrum of CopZ is not readily explained by the structure. All the conserved residues in this domain that do not coordinate the [2Fe-2S] cluster are located nearby. These include Tyr 76, Asn 113, Pro 114, and Cys 118. The side chains of Tyr 76 and Asn 113 point away from the [2Fe-2S] cluster towards a polar, 61 Å<sup>3</sup> cavity that contains ordered solvent and an acetate molecule derived from the crystallization solution (Fig. 5C). The [2Fe-2S] cluster forms the roof of this cavity. Such cavities are also observed in other [2Fe-2S] proteins such as *Trichomonas vaginalis* ferredoxin (55). The remaining conserved residue, Cys 118, lies on the protein surface 4 Å from [2Fe-2S] center and hydrogen bonds to a non-conserved histidine, His 120. The Cys118Ser mutant, however, binds as much copper as native CopZ, suggesting Cys 118 and His 120 do not constitute the additional copper binding site.

*Functional Implications.* CopZ from *A. fulgidus* is the first known fusion of a redox active [2Fe-2S]-containing domain to an Atx1-like CXXC-containing domain that delivers Cu<sup>+</sup> ions. The combination of these two modular units differentiates CopZ from all other members of the Atx1-like copper chaperone family. CopZ binds Cu<sup>+</sup> and can transfer it to the N-MBD of its putative partner Cu<sup>+</sup>-ATPase CopA, and likely has the same fold as and a similar function to other Atx1-like proteins. By

contrast, CopZ-NT has a novel fold and represents a new class of [2Fe-2S] protein that appears to be found only in extremophilic organisms. This domain is further partitioned into smaller units, each housing a metallo-cofactor. The exact role of CopZ-NT is unknown, but the presence of a [2Fe-2S] center strongly suggests that a redox function is involved.

One possibility is that the [2Fe-2S] cluster reduces Cu<sup>2+</sup> to Cu<sup>+</sup>. The Cu<sup>+</sup> might then bind to the CopZ-CT CXXC sequence for subsequent shuttling to the CopA N-MBD or the CopA transmembrane copper binding site for efflux. In support of this model, CopZ can reduce Cu<sup>2+</sup> to Cu<sup>+</sup>, and CopZ-NT binds one copper ion. It is conceivable that Cu<sup>2+</sup> binds transiently to a site near the [2Fe-2S] cluster (Fig. 5C), is reduced, and then transferred to the CopZ-CT. At present we are trying to identify the location of the Cu<sup>+</sup> binding site in the CopZ-NT and assess its possible role in metal transfer to the CopA MBDs.

Electrostatic surface calculations using PyMOL (56) reveal extended positively and negatively charged patches on the face of CopZ-NT containing [2Fe-2S] cluster (Fig. 6D). Homology modeling and electrostatic surface calculations for CopZ-CT (Figs. 5E and 5F) suggest that this domain has a negatively charged surface. These complementary surfaces could allow docking with the metal binding sites in close proximity and subsequent metal transfer between domains.

Several organisms, including *A. fulgidus* and *Enterococcus hirae*, express a Cu<sup>2+</sup>-ATPase, called CopB, that utilizes histidine-rich cytosolic metal binding domains to facilitate Cu<sup>2+</sup> removal (8,57,58). In *E. hirae*, CopB is co-transcribed with CopA in response to copper stress (59). As an additional or alternative route for Cu<sup>2+</sup> removal, *A. fulgidus* CopZ could reduce Cu<sup>2+</sup> to Cu<sup>+</sup>, allowing CopB and CopA to function simultaneously. Given that *A. fulgidus* is an anaerobic, sulfur-metabolizing hyperthermophile (60,61), is reasonable that its copper trafficking system differs from those in other organisms. Prior to the advent of an oxidizing atmosphere, copper was not an essential element (62), and the earliest copper ATPases probably only functioned in detoxification. Further characterization of *A. fulgidus* CopZ and its interactions with CopA may provide new insight into the evolution of copper homeostatic pathways.

## **Acknowledgements**

We thank M. González-Guerrero for his generous help with the Cu<sup>+</sup> transfer experiments.. Use of the Advanced Photon Source was supported by the United States Department of Energy, Office of Science, Office of Basic Energy Sciences under Contract No. DE-AC02-06CH11357.

## Footnotes

\*This work was supported by NIH grant GM58518 (A. C. R), NSF grant MCM-0235165 (J. M. A.), NIH grant HL13531 (B. M. H.), and NIH grant DK068139 (T. L. S.). M. H. S. was supported by NRSA Fellowship GM073457.

*The atomic coordinates (code 2HU9) have been deposited in the Protein Data Bank, Research Collaboratory for Structural Bioinformatics, Rutgers University, New Brunswick, NJ (<http://www.rcsb.org/>)*

<sup>1</sup>Abbreviations: A-domain, actuator domain; ATPBD, ATP binding domain; BCA, bicinchoninic acid; C-MBD, C-terminal CopA metal binding domain; CopZ-CT, CopZ C-terminus; CopZ-NT, CopZ N-terminus; HABA, 2-(4-hydroxyphenylazo)benzoic acid; MNK, Menkes syndrome protein; N-MBD, N-terminal CopA metal binding domain; r.m.s.d., root mean square deviation; SERCA1, sarcoplasmic reticulum Ca<sup>2+</sup>-ATPase; WND, Wilson disease protein.

## References

1. Rosenzweig, A. C. (2001) *Acc. Chem. Res.* **34**, 119-128
2. Huffman, D. L., and O'Halloran, T. V. (2001) *Annu. Rev. Biochem.* **70**, 677-701
3. Llanos, R. M., and Mercer, J. F. B. (2002) *DNA Cell Biol.* **21**, 259-270
4. Sarkar, B. (1999) *Chem. Rev.* **99**, 2535-2544
5. Bull, P. C., and Cox, D. W. (1994) *Trends Genet.* **10**, 246-252
6. Cox, D. W., and Moore, S. D. (2002) *J. Bioenerg. Biomembr.* **34**, 333-338
7. Hsi, G., and Cox, D. W. (2004) *Human Genet.* **114**, 165-172
8. Argüello, J. M. (2003) *J. Membr. Biochem.* **195**, 93-108
9. Axelsen, K. B., and Palmgren, M. G. (1998) *J. Mol. Evol.* **46**, 84-101
10. Lutsenko, S., and Kaplan, J. H. (1995) *Biochemistry* **34**, 15607-15613
11. Achila, D., Banci, L., Bertini, I., Bunce, J., Ciofi-Baffoni, S., and Huffman, D. L. (2006) *Proc. Natl. Acad. Sci. USA* **103**, 5729-5734
12. Banci, L., Bertini, I., Ciofi-Baffoni, S., Gonnelli, L., and Su, X. C. (2003) *J. Biol. Chem.* **278**, 50506-50513
13. Banci, L., Bertini, I., Ciofi-Baffoni, S., Huffman, D. L., and O'Halloran, T. V. (2001) *J. Biol. Chem.* **276**, 8415-8426
14. Gitschier, J., Moffat, B., Reilly, D., Wood, W. I., and Fairbrother, W. J. (1998) *Nature Struct. Biol.* **5**, 47-54

**Characterization and Structure of a Zn<sup>2+</sup> and [2Fe-2S]-Containing Copper Chaperone from *Archaeoglobus fulgidus* | Matthew Sazinsky, et. al**

15. Arnesano, F., Banci, L., Bertini, I., Huffman, D. L., and O'Halloran, T. V. (2001) *Biochemistry* **40**, 1528-1539
16. Banci, L., Bertini, I., Conte, R. D., Markey, J., and Ruiz-Dueñas, F. J. (2001) *Biochemistry* **40**, 15660-15668
17. Rosenzweig, A. C., Huffman, D. L., Hou, M. Y., Wernimont, A. K., Pufahl, R. A., and O'Halloran, T. V. (1999) *Structure* **7**, 605-617
18. Wernimont, A. K., Huffman, D. L., Lamb, A. L., O'Halloran, T. V., and Rosenzweig, A. C. (2000) *Nature Struct. Biol.* **7**, 766-771
19. Wimmer, R., Herrmann, T., Solioz, M., and Wüthrich, K. (1999) *J. Biol. Chem.* **274**, 22597-22603
20. Cobine, P. A., George, G. N., Winzor, D. J., Harrison, M. D., Mogahaddas, S., and Dameron, C. T. (2000) *Biochem.* **39**, 6857-6863
21. DiDonato, M., Hsu, H.-F., Narindrasorasak, S., Que, L., Jr., and Sarkar, B. (2000) *Biochem.* **39**, 1890-1896
22. Forbes, J. R., Hsi, G., and Cox, D. W. (1999) *J. Biol. Chem.* **274**, 12408-12413
23. Hamza, I., Schaefer, M., Klomp, L. W. J., and Gitlin, J. D. (1999) *Proc. Natl. Acad. Sci. USA* **96**, 13363-13368
24. Huffman, D. L., and O'Halloran, T. V. (2000) *J. Biol. Chem.* **275**, 18611-18614
25. Walker, J. M., Tsivkovskii, R., and Lutsenko, S. (2002) *J. Biol. Chem.* **277**, 27953-27959
26. Wernimont, A. K., Yatsunyk, L. A., and Rosenzweig, A. C. (2004) *J. Biol. Chem.* **279**, 12269-12276
27. Mandal, A. K., Cheung, W. D., and Argüello, J. M. (2002) *J. Biol. Chem.* **277**, 7201-7208
28. Sazinsky, M. H., Agarwal, S., Argüello, J. M., and Rosenzweig, A. C. (2006) *Biochemistry* **45**, 9949-9955
29. Sazinsky, M. H., Mandal, A. K., Argüello, J. M., and Rosenzweig, A. C. (2006) *J. Biol. Chem.* **281**, 11161-11166
30. Brenner, A. J., and Harris, E. D. (1995) *Anal. Biochem.* **226**, 80-84
31. Stookey, L. L. (1970) *Anal. Chem.* **42**, 779-781
32. Beinert, H. (1983) *Anal. Biochem.* **131**, 373-378
33. Cook, J. D., Bencze, K. Z., Jankovic, A. D., Crater, A. K., Busch, C. N., Bradley, P. B., Stemmler, A. J., Spaller, M. R., and Stemmler, T. L. (2006) *Biochemistry* **45**(25), 7767-7777
34. George, G. N., George, S. J., and Pickering, I. J. (2001) EXAFSPAK. In., <http://www-ssrl.slac.stanford.edu/~george/exafspak/exafs.htm>
35. Ankudinov, A. L., and Rehr, J. J. (1997) *Phys. Rev. B* **56**, R1712-R1715
36. Lieberman, R. L., Kondapalli, K. C., Shrestha, D. B., Hakemian, A. S., Smith, S. M., Telsler, J., Kuzelka, J., Gupta, R., Borovik, A. S., Lippard, S. J., Hoffman, B. M., Rosenzweig, A. C., and Stemmler, T. L. (2006) *Inorg. Chem.* **45**, 8372-8381
37. Lee, P. A., Citrin, P. H., Eisenberger, P., and Kincaid, B. M. (1981) *Rev. Mod. Phys.* **53**(4), 769-806

**Characterization and Structure of a Zn<sup>2+</sup> and [2Fe-2S]-Containing Copper Chaperone from *Archaeoglobus fulgidus* | Matthew Sazinsky, et. al**

38. Riggs-Gelasco, P. J., Stemmler, T. L., and Penner-Hahn, J. E. (1995) *Coord. Chem. Rev.* **144**, 245-286
39. Otwinowski, Z., and Minor, W. (1997) *Methods Enzymol.* **276**, 307-326
40. Terwilliger, T. C., and Berendzen, J. (1999) *Acta Cryst.* **D55**, 849-861
41. Brünger, A. T., Adams, P. D., Clore, G. M., DeLano, W. L., Gros, P., Grosse-Kunstleve, R. W., Jiang, J.-S., Kuszewski, J., Nilges, M., Pannu, N. S., Read, R. J., Rice, L. M., Simonson, T., and Warren, G. L. (1998) *Acta Cryst.* **D54**, 905-921
42. Cohen, S. X., Morris, R. J., Fernandez, F. J., Ben Jelloul, M., Kakaris, M., Parthasarathy, V., Lamzin, V. S., Kleywegt, G. J., and Perrakis, A. (2004) *Acta Cryst.* **D60**, 2222-2229
43. McRee, D. E. (1999) *J. Struct. Biol.* **125**, 156-165
44. Laskowski, R. A. (1993) *J. Appl. Cryst.* **26**, 283-291
45. Messerschmidt, A., Huber, R., Wieghardt, K., and Poulos, T. (eds). (2001) *Handbook of Metalloproteins*, John Wiley & Sons, New York
46. Mandal, A. K., and Argüello, J. M. (2003) *Biochemistry* **42**, 11040-11047
47. Yatsunyk, L. A., and Rosenzweig, A. C. (2007) *J. Biol. Chem.* **282**, 8622-8631
48. Lippard, S. J., and Berg, J. M. (1994) *Principles of bioinorganic chemistry*, University Science Books, Mill Valley
49. Solomon, E. I., Szilagyi, R. K., George, S. D., and Basumallick, L. (2004) *Chem. Rev.* **104**, 419-458
50. Westre, T. E., Kennepohl, P., DeWitt, J. G., Hedman, B., Hodgson, K. O., and Solomon, E. I. (1997) *J. Am. Chem. Soc.* **119**, 6297-6314
51. Davydov, A., Davydov, R., Gräslund, A., Lipscomb, J. D., and Andersson, K. K. (1997) *J. Biol. Chem.* **272**, 7022-7026
52. Holm, L., and Sander, C. (1993) *J. Mol. Biol.* **233**, 123-138
53. Hubbard, T. J. P., Murzin, A. G., Brenner, S. E., and Chothia, C. (1997) *Nucleic Acids Res.* **25**, 236-239
54. Sticht, H., and Rösch, P. (1998) *Prog. Biophys. Molec. Biol.* **70**, 95-136
55. Crossnoe, C. R., Germanas, J. P., LeMagueres, P., Mustata, G., and Krause, K. L. (2002) *J. Mol. Biol.* **318**, 503-518
56. DeLano, W. L. (2002) *The PyMOL molecular graphics system*, DeLano Scientific, San Carlos, CA
57. Bissig, K.-D., Wunderli-Ye, H., Duda, P. W., and Solioz, M. (2001) *Biochem. J.* **357**, 217-223
58. Mana-Capelli, S., Mandal, A. K., and Argüello, J. M. (2003) *J. Biol. Chem.* **278**, 40534-40541
59. Solioz, M., and Stoyanov, J. V. (2003) *FEMS Microbiol. Rev.* **27**(2-3), 183-195
60. Kletzin, A., Urich, T., Müller, F., Bandejas, T. M., and Gomes, C. M. (2004) *J. Bioenerg. Biomemb.* **36**, 77-91
61. Stetter, K. O. (1999) *FEBS Lett.* **452**, 22-25
62. Kaim, W., and Rall, J. (1996) *Angew. Chem. Int. Ed. Engl.* **35**, 43-60
63. Lund, O., Nielsen, M., Lundegaard, C., and Worning, P. (2002) *CASP5 conference*, A102